Processing and Characterization of Single-Crystalline Ultrafine Bismuth Nanowires

Zhibo Zhang,[†] Dmitry Gekhtman,[†] Mildred S. Dresselhaus,[†,‡] and Jackie Y. Ying*[,§]

Department of Physics, Department of Electrical Engineering and Computer Science, and Department of Chemical Engineering, Massachusetts Institute of Technology, Cambridge, Massachusetts 02139-4307

Received December 29, 1998. Revised Manuscript Received April 21, 1999

By pressure injecting Bi liquid melt into the nanochannels of an anodic alumina template, we have successfully fabricated Bi nanowire arrays with ultrafine wire diameters and extremely high wire packing densities. Free-standing Bi nanowires with controlled wire diameters and large aspect ratios (length/diameter) were also obtained by subsequent etching of the alumina template. Various techniques such as SEM, TEM, AFM, EFM, HREM, and XRD have been used to investigate the physical characteristics of these nanowires. The Bi nanowires were found to be dense and continuous and had a uniform diameter throughout the length of the wires. Individual Bi nanowires were shown to be single crystals, and all the wires in an array were highly oriented. An interesting metastable phase of Bi was also observed, which can be attributed to a lattice stress-induced high-pressure phase of Bi formed inside the porous anodic alumina template.

Introduction

Low-dimensional systems represent one of the important frontiers in advanced material research. Quantum confinement of electrons in low-dimensional systems provides a powerful tool for manipulating their optical, electrical and thermoelectric properties.[1−3] In recent years, significant progress has been made in two-dimensional (2D) quantum well systems and zero-dimensional (0D) quantum dot systems. However, the advancement in one-dimensional (1D) quantum wire systems has been slow due to the difficulties associated with fabricating such materials with controlled composition and characteristics. A few techniques have been developed to fabricate a variety of metal and semiconductor nanowires.[4−11] However, the resulting nanowires were either polycrystalline or their diameters have not reached the quantum confinement regime due to their large electron effective masses.

Recently, we developed a novel vacuum melting and pressure injection process to produce an array of ultrafine Bi nanowires embedded in a dielectric matrix.[12] Since Bi has the smallest electron effective mass among all known materials, quantum confinement effects in Bi are more pronounced and can be observed in nanowires of larger diameter than for any other nanowire systems. We have found strong evidence for quantum confinement effects in both the optical and magnetotransport properties of Bi nanowires,[12,13] which confirmed that these nanowires were truly a 1D system. The extremely small electron effective mass of Bi makes these nanowires an excellent system for studying the unique properties of a quasi-1D electron gas. Furthermore, our preliminary results[12] showed that the Bi nanowires are essentially single crystals, making this system very appealing for applications that could exploit the single crystallinity and/or anisotropy of Bi.

Here we report detailed investigations of the processing and characterization of Bi nanowire arrays and free-standing nanowires. The structure of the Bi/anodic alumina nanocomposite was examined with scanning electron microscopy (SEM) and transmission electron microscopy (TEM). The continuity of Bi nanowires embedded in the dielectric matrix was studied with scanning electrical field gradient microscopy (EFM) combined with atomic force microscopy (AFM). High-resolution electron microscopy (HREM) and X-ray diffraction (XRD) were employed to characterize the crystal structure of free-standing nanowires and nanowire arrays, respectively. Our studies showed that the Bi nanowires were dense and continuous and had a uniform diameter throughout their entire lengths, as

* To whom correspondence should be addressed.
[†] Department of Physics.
[‡] Department of Electrical Engineering and Computer Science.
[§] Department of Chemical Engineering.

(1) RodriguesViejo, J.; Jensen, K. F.; Mattoussi, H.; Michel, J.; Dabbousi, B. O.; Bawendi, M. G. *Appl. Phys. Lett.* **1997**, *70*, 2132.
(2) Pfeiffer, L.; Yacoby, A.; Stormer, H. L.; Baldwin, K. L.; Hasen, J.; Pinczuk, A.; Wegscheider, W.; West, K. W. *Microelectron. J.* **1997**, *28*, 817.
(3) Hicks, L. D.; Dresselhaus, M. S. *Phys. Rev. B* **1993**, *47*, 12727.
(4) Routekevitch, D.; Bigioni, T.; Moskovits, M.; Xu, J. M. *J. Phys. Chem.* **1996**, *100*, 14037. Routkevitch, D.; Haslett, T. L.; Ryan, L.; Bigioni, T.; Douketis, C.; Moskovits, M. *Chem. Phys.* **1996**, *210*, 343.
(5) Whitney, T. M.; Jiang, J. S.; Searson, P. C.; Chien, C. L. *Science* **1993**, *261*, 1316.
(6) Martin, C. R. *Science* **1994**, *266*, 1961. Martin, C. R. *Chem. Mater.* **1996**, *8*, 1739.
(7) Lakshmi, B. B.; Dorhout, P. K.; Martin, C. R. *Chem. Mater.* **1997**, *9*, 857.
(8) Huber, C. A.; Huber, T. E.; Sadoqi, M.; Lubin, J. A.; Manalis, S.; Prater, C. B. *Science* **1994**, *263*, 1961.
(9) Chakarvarti, S. K.; Vetter, J. *Radiat. Meas.* **1998**, *29*, 149.
(10) Wong, E. W.; Maynor, B. W.; Burns, L. D.; Lieber, C. M. *Chem. Mater.* **1996**, *8*, 2041.
(11) Morals, A. M.; Lieber, C. M. *Science* **1998**, *279*, 208.
(12) Zhang, Z. B.; Ying, J. Y.; Dresselhaus, M. S. *J. Mater. Res.* **1998**, *13*, 1745.
(13) Zhang, Z. B.; Sun, X. Z.; Dresselhaus, M. S.; Ying, J. Y.; Heremans, J. P. *Appl. Phys. Lett.* **1998**, *73*, 1589.

10.1021/cm9811545 CCC: $18.00
Published on Web 06/17/1999

desired for most transport-related applications. An interesting metastable phase was also observed in the XRD patterns of the as-prepared Bi nanowire arrays, which could be attributed to a lattice stress-induced high-pressure phase of Bi produced within the nanochannels of the template. In addition to the material characterization studies, this paper also presents a detailed description on the synthesis of these nanowires, elaborating on the procedures that were briefly discussed in our previous publication.[12]

Experimental Section

In this study, a template-assisted approach[12] was used to fabricate Bi nanowires. The template was porous anodic alumina, which was generated by anodizing a high-purity Al substrate (99.997%, Alfa AESAR) in acid solutions. Anodic alumina has an array of densely packed parallel nanochannels that are arranged in a hexagonal fashion, with a channel diameter and a packing density that can be systematically controlled by changing the processing parameters.[14−18] The channel packing density of anodic alumina depends mainly on the anodization voltage, while the channel diameter depends on the anodization voltage, the nature of the electrolyte, and the bath temperature. To obtain a uniform porous structure in the resulting anodic alumina film, the starting Al substrate was mechanically polished with a 3-μm diamond paste, followed by Mastermate (Buehler), which is an aqueous dispersion of fine SiO_2 particles with an average particle size of ~20 nm. The substrate was then annealed at 350 °C for 1 h in air, before it was further electrochemically polished for a couple of minutes in a mixed acidic solution of 95 vol % H_3PO_4 (85%, Alfa AESAR) and 5 vol % H_2SO_4 (97%, Alfa AESAR) plus 20 g/L CrO_3. The temperature of the solution was maintained at 84 ± 2 °C, and the polishing voltage was ~20 V. The polished Al substrate was dipped into a solution of 3.5 vol % H_3PO_4 and 45 g/L CrO_3 at 90 °C for several minutes to dissolve the oxide layer on the Al surface right before the anodization process. Depending on the channel diameter desired, the Al substrate was anodized in an electrolyte solution of 20 wt % H_2SO_4 or 4 wt % $H_2C_2O_4$. The pore diameter of the anodic alumina film can subsequently be adjusted by etching the as-anodized template in a second acid solution. For templates anodized in a 4 wt % $H_2C_2O_4$ electrolyte (denoted as C-templates), a 5 wt % H_3PO_4 solution was used as the etching agent; while for templates anodized in a 20 wt % H_2SO_4 electrolyte (denoted as S-templates), a 20 wt % H_2SO_4 solution was used in the pore-enlargement etching. In this study, average channel diameters of 20−120 and 9−30 nm were achieved for C-templates and S-templates, respectively. The highest channel packing density was $\sim 7 \times 10^{10}$ cm^{-2}, and channel lengths (or template thickness) were controlled by the anodization period to be 20−60 μm. The well-defined porous structure and the large band gap of anodic alumina make it an excellent material for matrix-mediated synthesis and hosting of nanowires.

The as-prepared porous anodic alumina template was washed extensively with deionized water and dried in air. To stabilize the template, the sample was calcined at 350 °C for 2 h in air before the vacuum melting and pressure injection process. The anodic alumina template, which was still attached to the Al substrate, was then placed on the bottom of a glass beaker and surrounded with high-purity (99.999%) Bi pieces. Since Bi has a high mass density, two long Al wires were placed across the template to keep the template on the bottom of the beaker and to prevent it from floating to the surface of liquid Bi after Bi has been melted. Al wires were used here because Al has essentially zero solubility in liquid Bi at the temperatures ($T \leq 325$ °C) used for the pressure injection of liquid Bi. The glass beaker containing the template and Bi pieces was then placed inside a high-pressure inconel reactor with gas inlet and outlet valves. To degas the nanochannels of the template, the reactor chamber was evacuated to $\sim 10^{-2}$ mbar for 8 h at 250 °C, which was below the melting point of Bi (271.5 °C). After degassing, the chamber was heated to 325 °C. The Bi pieces were melted by that temperature, and the template was immersed in the liquid melt. The vacuum pump was then disconnected from the chamber, and high-pressure Ar gas (~4500 psi) was introduced into the chamber to inject liquid Bi into the nanochannels of the template for a period of 5 h. The chamber was then slowly cooled to room temperature over a period longer than 12 h. During the cooling process, the impregnated Bi was solidified and crystallized inside the nanochannels. The slow cooling process was found to be critical for generating single-crystalline Bi nanowires. The high-pressure Ar gas was then slowly released.

This fabrication process was also modified to incorporate Te dopants into the Bi nanowires. We prepared 0.1 atom % Te-doped Bi nanowire samples by substituting pure Bi pieces with $Bi_{0.999}Te_{0.001}$ alloy for the vacuum melting/pressure injection process. The electronic transport properties of the n-type Te-doped Bi nanowires were found to be different from those of pure Bi nanowires, and the results will be reported elsewhere. It is conceivable that other types of dopants from columns IV and VI of the periodic table can also be incorporated into the Bi nanowires by this approach.

After the pressure injection process, the Bi-filled template was buried within the solidified Bi pieces and was mechanically recovered. Leaving the anodic alumina template on the Al substrate greatly reduced the difficulties in the sample retrieval. The Al substrate was then etched away with a solution of 0.2 M $HgCl_2$. The subsequently exposed alumina barrier layer,[14,15] which capped the ends of the nanochannels of the anodic alumina template, was etched away using 5 wt % H_3PO_4 and 20 wt % H_2SO_4 for C-templates and S-templates, respectively. The etching time depends on the thickness of the barrier layer, which was governed by the anodization voltage.[14,15]

To generate free-standing Bi nanowires, we developed an etching solution that would only dissolve the anodic alumina matrix at room temperature without affecting the Bi nanowires. The etching solution consists of 3.5 vol % H_3PO_4 and 45 g/L CrO_3. After the template was thoroughly dissolved and free-standing Bi nanowires were collected at the bottom of the container, the upper portion of the etching solution was removed with a pipet. Deionized water was then added to dilute the remaining etching solution. After this procedure was repeated for several times, the deionized water was replaced with 2-propanol. The Bi nanowire dispersion was then sonicated until the nanowires were well-dispersed in the organic solvent.

The Bi nanowire arrays and free-standing Bi nanowires were characterized using SEM, TEM, AFM, EFM, and XRD techniques. SEM studies were performed on a JEOL 6320 high-resolution scanning electron microscope, TEM studies were conducted using either a JEOL 200 CX or a Topcon 002B high-resolution transmission electron microscope operating at 200 kV. AFM and EFM investigations were carried out on a Digital Instruments Dimension 3000 scanning probe microscope. XRD studies were carried out on a Siemens D5000 $\theta-\theta$ X-ray diffractometer.

Results and Discussions

Since liquid Bi has a high surface tension (~375 dyn/cm), a high pressure was needed to force liquid Bi into the nanochannels of anodic alumina templates. Here the simplified Washburn equation,[19] $P = -4\gamma \cos\theta/d$, could

(14) Keller, F.; Hunter, M. S.; Robinson, D. L. *J. Electrochem. Soc.* **1953**, *100*, 411.
(15) Randon, J.; Mardilovich, P. P.; Govyadinov, A. N.; Paterson, P. *J. Colloid Interface Sci.* **1995**, *169*, 335.
(16) Ono, S.; Masuko, N. *Corros. Sci.* **1992**, *33*, 503.
(17) Masuda, H.; Yamada, H.; Sutoh, M.; Asoh, H.; Nakao, M.; Tamamura, T. *Appl. Phys. Lett.* **1997**, *71*, 2770.
(18) Li, F. Y.; Zhang, L.; Metzger, R. M. *Chem. Mater.* **1998**, *10*, 2470.

be used to estimate the external pressure P needed to fill a channel of diameter d, where γ is the surface tension of liquid Bi, and θ is the contact angle between the liquid Bi and the channel walls of the anodic alumina template. Since the equipment that we used could only sustain pressures up to 5000 psi, we can calculate with the above equation that the smallest channel diameter that can be filled at the maximum operating pressure is about 45 nm without use of any wetting agent. To fill channels with smaller diameters, we need to reduce either γ or θ. We found experimentally that the channels of S-templates were much easier to be filled by liquid Bi than those of C-templates. For instance, under a pressure of 4500 psi, channels with diameters as small as 13 nm in a S-template could be filled by liquid Bi, while the smallest channels that could be filled were about 50 nm in diameter for a C-template. This difference might be attributed to the different surface compositions of the templates prepared in different electrolytes. It has been known that anions from the electrolyte solution could be incorporated into the anodic alumina during the anodization process, with anion incorporations concentrated near the channel wall.[15,16] The different types of anions incorporated into the anodic alumina matrix could result in different surface chemistries of the channel walls. Since SO_4^{2-} can form a strong chemical bond with Bi,[20] this anion could lead to a reduced contact angle θ between the liquid Bi and the anodic alumina template. In contrast, the chemical bonding energy is smaller between the $C_2O_4^{2-}$ anion and the Bi atom. This might be one possible reason the channels of the S-templates were easier to be filled with liquid Bi than those of the C-templates.

While S-templates were easier to be filled with Bi, a method that can assist the filling of C-templates with liquid Bi is also desirable since it is difficult to produce S-templates with channel diameters larger than 30 nm and since C-templates typically have better structural uniformity than S-templates. In our experiments, we found that by introducing Cu impurities into liquid Bi, the filling factor of Bi in the C-templates could be dramatically increased compared to that when pure Bi was used. For instance, without Cu impurities, only about 10% of the channels in a C-template with an average channel diameter of 56 nm were filled by Bi at a pressure of 4500 psi. With Cu impurities incorporated in the liquid Bi, more than 90% of the channels of a similar C-template were filled. One possible reason for the increased filling factor might be the reduction of surface tension of Bi melt in the presence of Cu impurities.[21] Here Cu impurities were used because Cu has a small solubility in liquid Bi (~0.2 atom % at 325 °C), and essentially zero solubility in a solid Bi crystal. When liquid Bi crystallized, Cu atoms were segregated to the surface of the Bi crystal because of their lower density, thereby leaving pure Bi crystals inside the nanochannels of the template. Consequently, the resulting Bi nanowires have a high purity, and their electrical properties should not be affected much by this processing approach.

(19) Washburn, E. W. *Phys. Rev.* **1921**, *17*, 273.
(20) Lide, D. R. *CRC Handbook of Chemistry and Physics*; CRC Press: Boston, MA, 1998.
(21) Savov, L.; Heller, H. P.; Janke, D. *Metall* **1997**, *51*, 475.

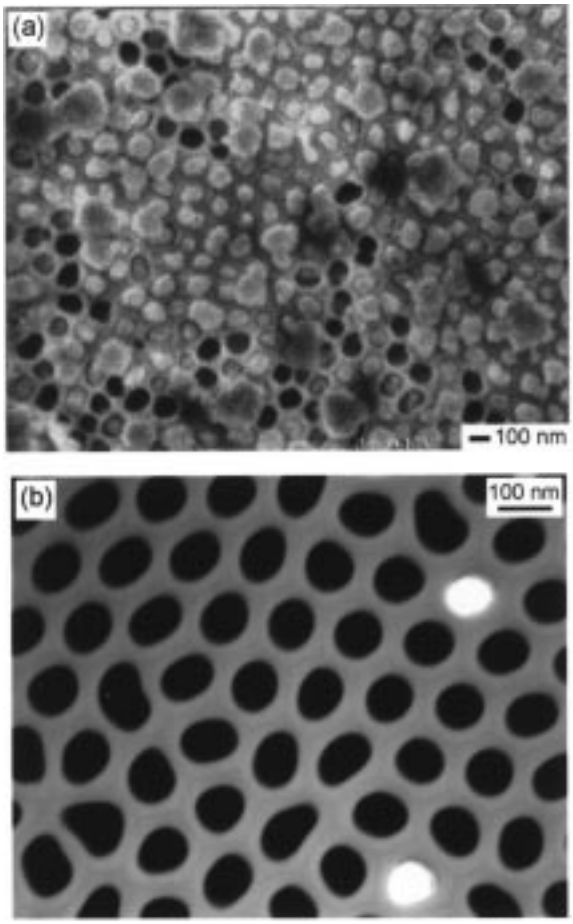

Figure 1. (a) SEM image of a Bi nanowire array with an average wire diameter of 109 nm, taken from the bottom surface after the barrier layer had been removed. The bright spots are Bi nanowires, while the dark spots are empty channels. (b) TEM image of the cross-section of a Bi nanowire array with an average wire diameter of 65 nm, taken after ion milling (Ar ions) at 6 keV. Here the dark spots are Bi nanowires, and the white spots are empty channels.

To verify that Bi has filled the nanochannels of the template all the way from the entrance to the end, we took SEM pictures of the bottom surface of the Bi nanowire arrays after the barrier layer has been removed. Shown in Figure 1a is one of such images, which was taken from a nanowire array with an average wire diameter of 109 ± 24 nm. We note that more than 90% of the channels of the portion of the sample shown have been filled by Bi. For templates with smaller channel diameters, the fraction of the channels that were filled by Bi was typically smaller. This is understandable, since it is more difficult to fill the channels with liquid Bi under the same pressure when the channel diameter is smaller. Furthermore, with smaller channel diameters, the chance that a channel is blocked by impurities may increase, thereby preventing the proper filling of the channel by liquid Bi. To examine the internal structure of the Bi nanowire array, the anodic alumina/Bi nanowire composite was milled from both sides of the thin film using 6 keV Ar ions. Figure 1b shows a TEM image of the cross-section of a Bi nanowire array with an average wire diameter of 65 ± 8 nm prepared with a C-template. Since Bi has a higher density than anodic alumina, it is shown in dark contrast in the TEM image.

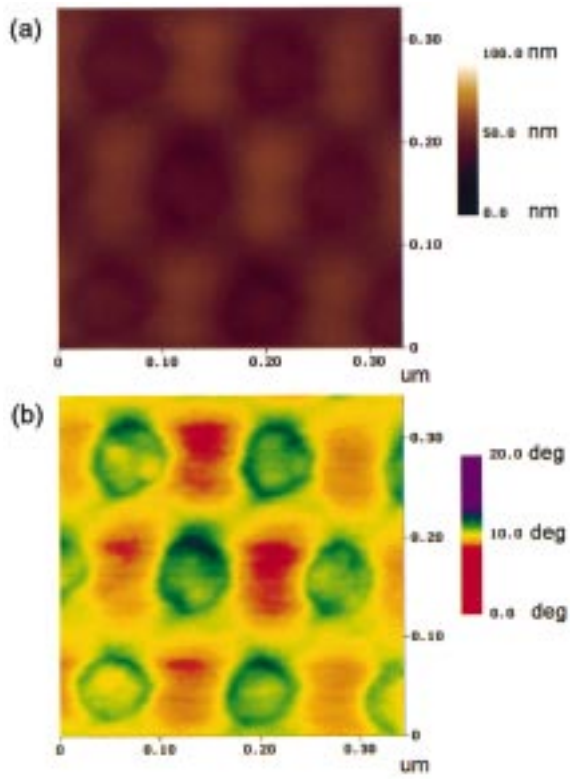

Figure 2. (a) AFM topographical image of a Bi nanowire array with an average wire diameter of 65 nm, taken after the surface was sputtered with 6 keV Ar ions. (b) EFM image of the same portion of the Bi nanowire array shown in part a. A small electrical field gradient is shown in red or yellow, as opposed to green or purple for a large electrical field gradient.

We also used a scanning probe microscope working in the electrical field gradient microscopy (EFM) mode[8,22] to investigate the continuity of individual Bi nanowires embedded in the dielectric matrix. First, the top surface of a Bi nanowire array (consisting of a thin Bi layer connecting to individual nanowires) was mounted to a metal substrate using a conducting silver paint. The bottom surface of the Bi nanowire array was then milled by Ar ions to generate a smooth surface for EFM measurements. During the EFM experiment, a bias voltage (-2 V $< V_b <$ 2 V) was applied between the metal substrate and the scanning cantilever tip. The conducting silicon tip, which has a diameter of about 10 nm, scanned the sample surface twice.[23] In the first scan, the machine was working in the tapping mode and the tip remained at a constant distance (only a few nanometers) away from the sample surface, and a topographic image of the surface was obtained (Figure 2a). Since the sample surface after ion milling was very flat, as shown in the AFM image, there was little contrast between the Bi nanowires and the anodic alumina matrix. In the second scan, the scanning tip followed the same movement of the first scan, so that the tip was moving at the same constant distance from the sample surface. The difference in the vertical electrical field gradient of the sample surface resulted in different resonance frequency of the tip, which was recorded and was used to generate the EFM image of the sample surface (Figure 2b). This technique provided a lateral resolution finer than 5 nm, and allowed surface charge detection with an accuracy of a single electron charge.[23] Since the anodic alumina matrix was insulating, it generated a very small electrical field gradient on the surface, corresponding to the red or yellow portions of the image. A continuous metallic Bi nanowire would induce a large electrical field gradient on the surface, illustrated as green or purple in the color scale of the EFM image. On the other hand, if a Bi nanowire is not continuous, the electrical field gradient on the surface would be small, yielding an image with color similar to that of the insulating matrix. Figure 2 illustrates that the Bi nanowires were continuous within the channels of the template. Such continuity along individual nanowires is a critical requirement for most transport-related applications.

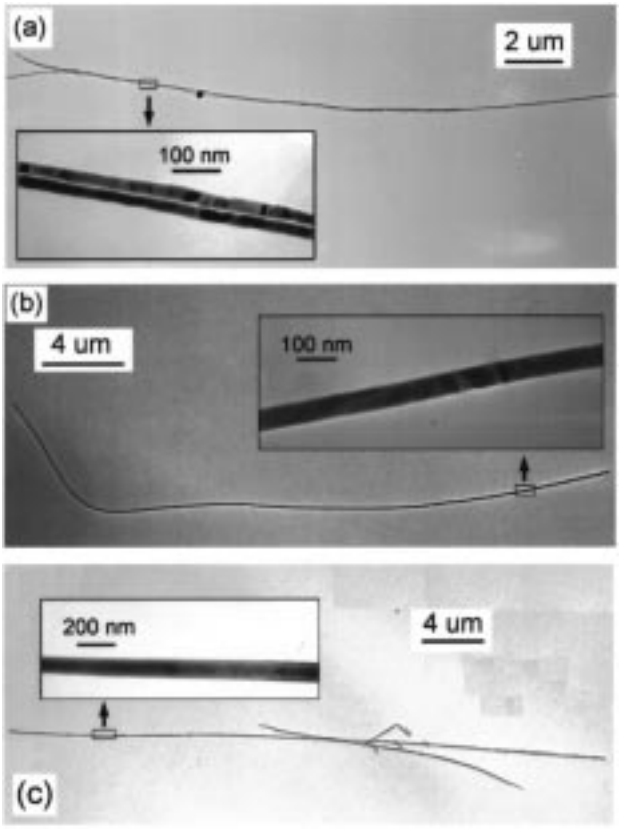

Figure 3. TEM images of long free-standing Bi nanowires with wire diameters of (a) 23 nm, (b) 65 nm, and (c) 109 nm. The insets show the high-magnification images taken from a portion of the long wires.

Transmission electron microscopy (TEM) and high-resolution electron microscopy (HREM) were employed to study the free-standing Bi nanowires after the anodic alumina matrix had been thoroughly dissolved. TEM samples were prepared by transferring a small drop of the Bi nanowire dispersion to TEM grids covered with a thin carbon film. Although many of the free-standing Bi nanowires on the TEM grid were found to be shorter than 10 μm, some long nanowires were observed with lengths almost equal to the film thickness of the template. This distribution in wire lengths existed because Bi is a soft material, and its nanowires could be easily broken during the dispersion process. Shown in Figure 3 are TEM images of some of the long Bi nanowires with various wire diameters. Figure 3a

(22) Martin, Y.; Abraham, D. W.; Wickramasinghe, H. K. *Appl. Phys. Lett.* **1988**, *52*, 1103.
(23) *Dimension 3000 Operation Manual*; Digital Instruments: Santa Babara, CA.

actually shows two Bi nanowires with a wire diameter of about 23 nm, and a higher magnification image taken from a portion of the same wires is shown as the inset. The two wires are separated from each other at the left portion of the image. Figure 3b illustrates a single Bi nanowire with a wire diameter of about 65 nm, and Figure 3c shows several nanowires with an average wire diameter of 109 nm. The Bi nanowires are noted to have uniform wire diameters throughout the entire lengths of the wires. The uniform wire diameter is also an important characteristic for nanowires in transport-related applications, since the transport properties of a nanowire may be dominated by the portion of the wire with the smallest diameter. We note that for the image shown in the inset of Figure 3a, the sharp contrast along Bi nanowires was caused by the electron charging during the TEM experiment, not due to mass density changes within the nanowires. The continuity of the nanowires has been verified by HREM studies. With the small electron effective mass of Bi, these free-standing nanowires may provide an excellent system for studying the properties of quasi-1D electron gases, and techniques[24,25] recently developed for studying carbon nanotubes can also be employed to study our free-standing Bi nanowires.

The lattice fringes of the Bi nanowires can be observed in HREM images, as shown in Figure 4, parts a and b. We found that the Bi nanowires were essentially single crystals, and no grain boundaries were observed within the nanowires in the HREM studies. The single crystallinity of Bi nanowires was consistent with our previously published X-ray diffraction results[12] and was also confirmed by selected-area electron diffraction (SAED) experiments. Parts b and c of Figure 5 present the SAED patterns taken from two different single free-standing Bi nanowires. We always observed a single set of diffraction spots in all SAED patterns, indicating that individual Bi nanowires are truly single crystals. The single crystallinity of Bi nanowires is also an important characteristic for transport-related applications, especially for thermoelectric applications, where high carrier mobility is highly desirable. Furthermore, we found that Bi nanowires were very stable when they remained inside the channels of the anodic alumina template. For instance, the free-standing Bi nanowires shown in Figure 3a and Figure 4 were obtained from samples prepared about a year ago, and no difference was found in their structures compared to nanowires obtained from freshly prepared samples. However, free-standing Bi nanowires would gradually oxidize when exposed to air. Figure 4a shows a Bi nanowire that has been exposed to air for ~4 h, and the oxide layer on the wire surface is almost undetectable (<1 nm thick). In comparison, the Bi nanowires shown in Figures 4b and 5a had been exposed to air for 48 h before the TEM images were taken; the micrographs indicated that the oxide layer was thicker (~4 nm). After free-standing Bi nanowires had been exposed to air for more than 4 weeks, they were found to have become fully oxidized.

The crystal orientations of Bi nanowire arrays were investigated by X-ray diffraction (XRD) with the reflection plane perpendicular to the wire axis. Before the XRD experiment was performed, the excess Bi particles that were stuck to the sample surface were polished away using a 50-nm γ-Al_2O_3 polishing agent, and the alumina barrier layer was also removed to expose the ends of Bi nanowires. Parts b and d of Figure 6 show typical XRD patterns of the Bi nanowire arrays fabricated with C-templates after the samples were annealed at 200 °C for 8 h under flowing N_2. While bulk Bi has a rhombohedral crystal structure, the XRD patterns of the Bi nanowire arrays (Figure 6, parts b and d) only show three strong diffraction peaks. By normalizing the peak areas to the peak intensities of a polycrystalline bulk Bi standard, we found that more than 90% of the wires were oriented along a direction perpendicular to the (202) lattice plane for both nanowire arrays. This crystal orientation was the same as that observed in larger Bi microwires prepared in glass microtubes.[26,27] For Bi nanowire arrays prepared with S-templates, we observed two distinct preferential crystal orientations (Figure 7). Figure 7a shows a XRD pattern with a preferential orientation perpendicular to the (012) lattice plane, while Figure 7b presents a XRD pattern similar to that of the nanowire arrays prepared with C-templates. The origin of these different preferential crystal orientations obtained with S-templates is not

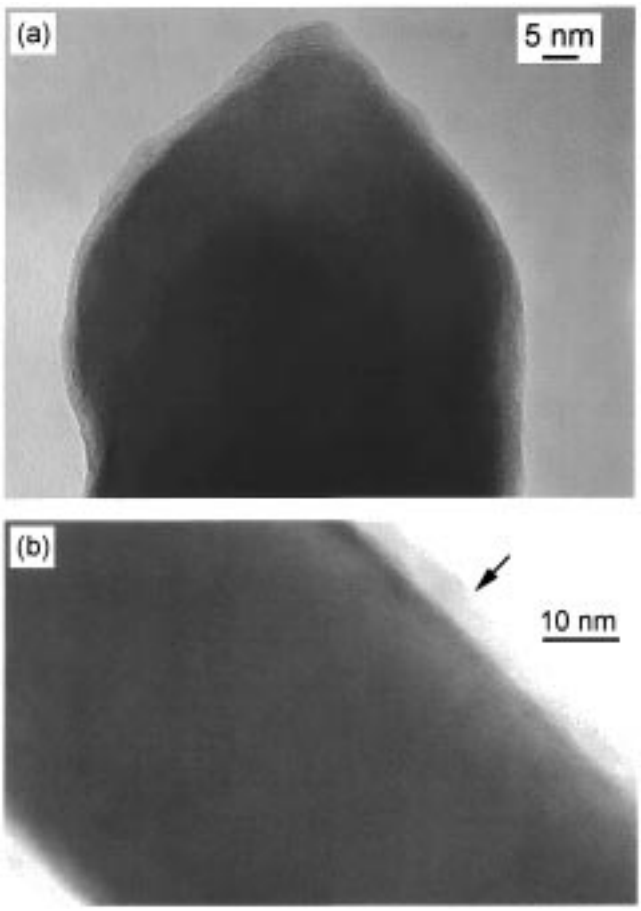

Figure 4. HREM images of different free-standing Bi nanowires with a wire diameter of 65 nm, showing lattice fringes. The arrow in part b points to the amorphous oxide layer on the wire surface.

(24) Ebbesen, T. W.; Lezec, H. J.; Hiura, H.; Bennett, J. W.; Ghaemi, H. F.; Thio, T. *Nature* **1996**, *382*, 54.
(25) Wildoer, J. W. G.; Venema, L. C.; Rinzler, A. G.; Smalley, R. E.; Dekker, C. *Nature* **1998**, *391*, 59.
(26) Brandt, N. B.; Gitsu, D. B.; Dolma, V. A.; Ponomarev, Y. G. *Sov. Phys. JETP* **1987**, *65*, 515.
(27) Gurtvich, M. *J. Low Temp. Phys.* **1980**, *38*, 777.

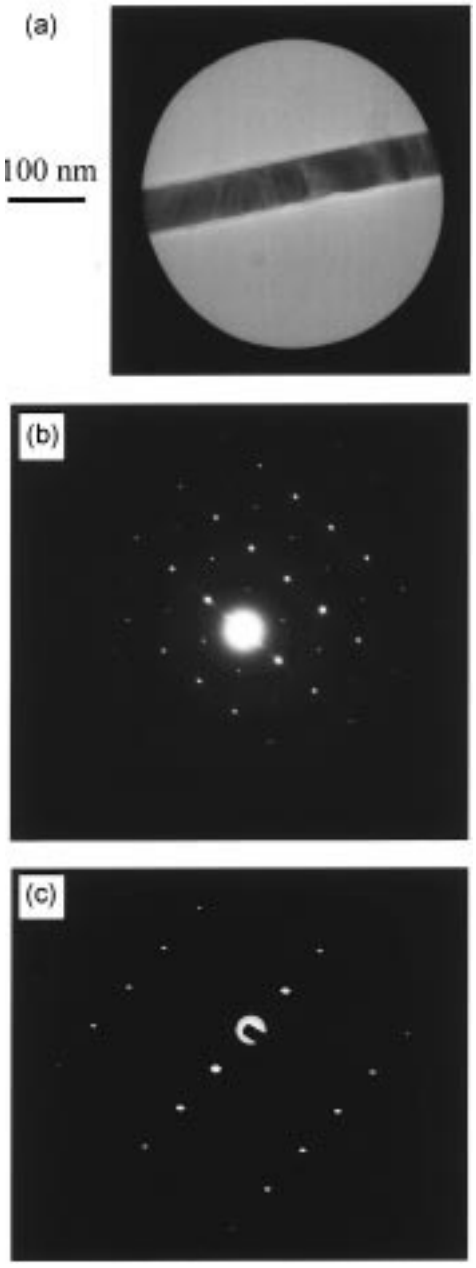

Figure 5. (a) TEM image of a small portion of a Bi nanowire, illustrating the aperture for the SAED experiment; the amorphous Bi oxide layer on the wire surface is clearly seen. (b and c) SAED patterns taken from different single free-standing Bi nanowires; in each case, the single set of electron diffraction spots corresponds to a single crystal of Bi.

currently understood, but it may be linked to the different seeds available in the liquid Bi bath during crystallization. From the results of the XRD experiments, as well as the HREM and SAED studies presented earlier, we conclude that individual Bi nanowires are single crystals and all nanowires in an array are highly oriented. Except for a small peak near the (202) peak in the XRD pattern of Figure 6d, all other intense XRD peaks were located at exactly the same positions as the polycrystalline Bi standard, indicating that the rhombohedral crystal structure of bulk Bi was preserved in the ultrafine nanowires. This has an important implication for Bi nanowires in transport-related applications, since it means that the unique properties of bulk Bi, such as its extremely small electron effective

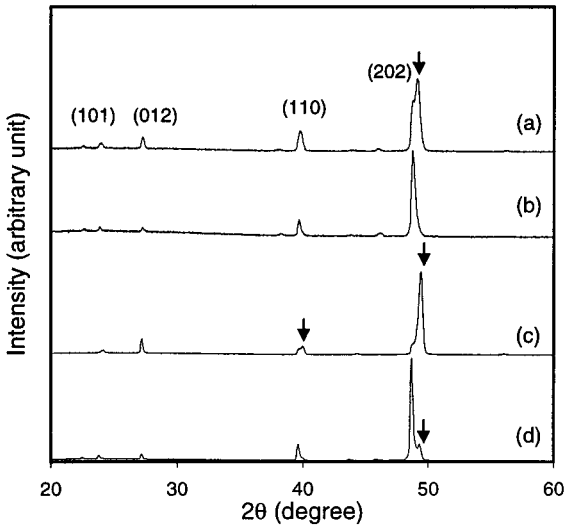

Figure 6. XRD patterns of the anodic alumina/Bi nanowire composites prepared with the C-templates, before and after the composites were thermally annealed at 200 °C for 8 h under flowing N_2: (a) as-prepared and (b) thermally annealed sample with an average wire diameter of 109 nm; (c) as-prepared and (d) thermally annealed sample with an average wire diameter of 65 nm. The arrows point to peaks of the metastable phase, while marked above the individual peaks are Miller indices corresponding to the lattice planes of bulk Bi.

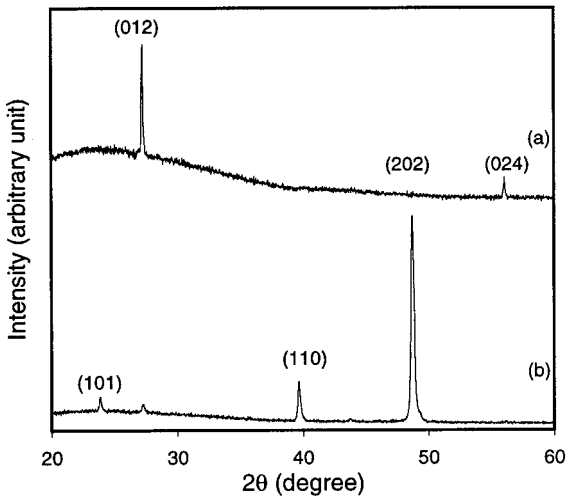

Figure 7. XRD patterns of the anodic alumina/Bi nanowire composites prepared with the S-templates, taken before thermal annealing. Both samples have an average wire diameter of about 23 nm. Marked above the individual peaks are Miller indices corresponding to the lattice planes of bulk Bi. The XRD peaks of both samples appear at the same positions as those of the polycrystalline Bi standard.

mass and the high anisotropy of its Fermi surface, are preserved in the ultrafine Bi nanowires.

In the XRD experiments, we also observed an interesting metastable phase in the as-prepared Bi nanowire arrays. Shown in Figure 6, parts a and c, are XRD patterns for two as-prepared Bi nanowire arrays with average wire diameters of 109 ± 24 nm and 65 ± 9 nm, respectively, both prepared using C-templates. We note that the major peaks of these two XRD patterns were shifted toward higher angles compared to the peak positions of the polycrystalline Bi standard. The shifts from the (202) peak position of bulk Bi were about 0.67° (2θ) and 0.40° (2θ) for the 65- and 109-nm nanowire

arrays, respectively. Although these peaks were stable at room temperature, they were not stable under thermal treatment. After the samples were annealed at 200 °C for 8 h under flowing N_2, the major peaks were found to shift back to the peak positions of the Bi standard as shown in Figure 6, parts b and d. The metastable peak for the 109-nm nanowire array essentially disappeared upon thermal annealing, while those for the 65-nm nanowire array underwent significant reduction in intensities after thermal treatment. For the Bi nanowire arrays whereby most of the wires were not extended all the way to the bottom surface of the template, metastable peaks were not noted (as in Figures 7, parts a and b).

The metastable phase observed in some of the nanowire arrays was very likely a high-pressure phase of Bi. It has been previously observed in Shubnikov−de Haas effect measurements that the extremal cross-sectional areas of both the electron and hole ellipsoids of bulk Bi decrease almost linearly with external pressure,[28] and the lattice constant of bulk Bi shrinks when an external pressure is applied.[29] In our system, since the Bi nanowires inside the channels of an anodic alumina template were crystallized under ~4500 psi, this external pressure might have an even more significant effect on the lattice constant of Bi nanowires than the same pressure applied to an already solidified Bi crystal. More importantly, in contrast to most other materials, Bi expands by 3.26% during its transition from liquid to solid.[20] This phase transition should exert an even greater pressure on the solidified Bi nanowires, since there was no free space into which the Bi could expand within the nanochannels of the template. Due to the confinement of the channel walls, the high stress induced on the Bi nanowire crystals should remain even when the external pressure has been released. This could explain our observation that the metastable peaks in the as-prepared nanowire arrays were found at higher diffraction angles than the (202) peak position of the Bi standard, which correspond to smaller lattice constants. After the barrier layer was removed, the lattice stress should be released during thermal annealing under ambient pressure. This would explain the reduction in intensities of the metastable peaks and the increased intensities of the standard Bi peaks after the samples have been thermally annealed. The high-pressure phase theory can also explain the differences in the peak shifts and peak intensity changes between the two samples of different wire diameters. In a C-template with a smaller channel diameter, the Bi nanowires would be more confined with less space for expansion during the liquid−solid phase transition. Therefore, the Bi lattice stress should be higher in a 65-nm nanowire array than in a 109-nm nanowire array. This would explain our observation that the magnitude of the peak shift was larger in the 65-nm sample than that in the 109-nm sample. Similarly, the release of lattice stress is also more difficult in a channel of smaller diameter; this would explain why after the thermal treatment, the metastable phase in the 109-nm sample essentially disappeared, but was still observable in the 65-nm sample. For samples prepared with the S-templates (Figure 7, parts a and b), whereby Bi did not thoroughly fill the nanochannels, the pressure on the solidifying Bi nanowires should be much smaller with the availability of free space for expansion during solidification. This would explain the absence of any metastable phase in Figure 7, parts a and b.

Without thermal treatment, the metastable high-pressure phase in the nanowire arrays could be stable for at least several months under ambient condition. Some researchers have previously proposed obtaining high-pressure phases inside a carbon nanotube.[30] This study demonstrated that high-pressure phases could be attained via pressure injection of Bi into a nanochannel template.

Summary

In summary, by pressure injection of Bi liquid melt into the evacuated nanochannels of an anodic alumina template, we have successfully fabricated Bi nanowire arrays with controlled wire diameters (13−110 nm) and extremely high packing densities (as high as 7×10^{10} cm^{-2}). Free-standing Bi nanowires with very large aspect ratios (on the order of several hundreds) have also been obtained by dissolving the anodic alumina matrix without affecting the Bi nanowires. The structures of Bi nanowire arrays and free-standing nanowires have been investigated by various characterization techniques. The Bi nanowires were shown to be dense and continuous, with a uniform wire diameter throughout their entire lengths. Individual nanowires were essentially single crystals, and the nanowires in an array were highly oriented. These excellent structural characteristics, in combination with the extremely small electron effective mass and low thermal conductivity of Bi, make our Bi nanowires especially promising for thermoelectric applications.[3] The free-standing Bi nanowires also provide an excellent system for studying the fundamental physics of a quasi-1D electron gas. Furthermore, an interesting Bi metastable phase was observed in the nanowire arrays, and could be attributed to a lattice stress-induced high-pressure phase of Bi. Considering the high thermal stability and chemical stability of the anodic alumina templates, the fabrication process that we have developed can be flexibly applied to other metals and semiconductors of low melting points for the synthesis of a variety of nanowire systems for different applications.

Acknowledgment. This project is partially funded by the National Science Foundation (DMR-9400334 and DMR-9510093), U.S. Navy (N00167-92-K0052) and MURI (Subcontract No. 0205-6-7A114-01). We thank Dr. D. Adderton of Digital Instruments for his assistance in AFM and EFM studies, Dr. G. Dresselhaus and M. L. Panchula of MIT and Dr. J. P. Heremans of General Motors R&D Center for valuable discussions.

CM9811545

(28) Itskevich, E. S.; Fisher, L. M. *Sov. Phys. JETP* **1968**, *26*, 66. Brandt, N. B.; Moshchalkov, V. V.; Chudinov, S. M. *Sov. Phys. JETP* **1977**, *45*, 953.

(29) Morosin, B.; Schirber, J. E. *Phys. Lett.* **1969**, *30A*, 512. Perez, E. E. M. Ph.D. Thesis, Department of Physics, Massachusetts Institute of Technology, Cambridge, MA, 1979.

(30) Ajayan, P. M.; Iijima, S. *Nature* **1993**, *361*, 33.